A second order in time, decoupled, unconditionally stable numerical scheme for the Cahn-Hilliard-Darcy system

Daozhi Han*, Xiaoming Wang†

August 31, 2016

Abstract

We propose a novel second order in time, decoupled and unconditionally stable numerical scheme for solving the Cahn-Hilliard-Darcy (CHD) system which models two-phase flow in porous medium or in a Hele-Shaw cell. The scheme is based on the ideas of second order convex-splitting for the Cahn-Hilliard equation and pressure-correction for the Darcy equation. We show that the scheme is uniquely solvable, unconditionally energy stable and mass-conservative. Ample numerical results are presented to gauge the efficiency and robustness of our scheme.

Keywords— Cahn-Hilliard-Darcy; diffuse interface model; energy law; unconditional stability; pressure-correction; decoupling

1 Introduction

For two-phase incompressible flows in porous medium or in a Hele-Shaw cell, a popular diffuse interface model is the Cahn-Hilliard-Darcy system, see for instance [27, 28, 42]. In this contribution, we consider solving numerically

*Department of Mathematics, Indiana University, Bloomington, IN 47405, USA. Email: *djhan@iu.edu*

†Department of Mathematics, Florida State University, Tallahassee, FL 32306, USA. Email: *wxm@math.fsu.edu*

a slightly different version of the Cahn-Hilliard-Darcy (CHD) system

$$\frac{ReDa}{\chi}\frac{\partial \mathbf{u}}{\partial t} + \alpha(\phi)\mathbf{u} = -\nabla p - \frac{\epsilon^{-1}}{We^*}\phi\nabla\mu, \text{ in } \Omega, \tag{1}$$

$$\nabla \cdot \mathbf{u} = 0, \text{ in } \Omega, \tag{2}$$

$$\chi\frac{\partial \phi}{\partial t} + \nabla \cdot (\phi\mathbf{u}) = \frac{1}{Pe}\nabla \cdot (m(\phi)\nabla\mu), \text{ in } \Omega, \tag{3}$$

$$\mu = \phi^3 - \phi - \epsilon^2\Delta\phi, \text{ in } \Omega, \tag{4}$$

$$\mathbf{u}|_{t=0} = \mathbf{u}_0, \quad \phi|_{t=0} = \phi_0, \text{ in } \Omega, \tag{5}$$

$$\mathbf{u} \cdot \mathbf{n} = 0, \quad \partial_{\mathbf{n}}\phi = 0, \quad \partial_{\mathbf{n}}\mu = 0, \text{ on } \partial\Omega. \tag{6}$$

Here Ω is a domain in $\mathbb{R}^2$ or $\mathbb{R}^3$ with Lipschitz continuous boundary $\partial\Omega$. $\mathbf{n}$ is the unit outer normal of the boundary $\partial\Omega$, and $\partial_{\mathbf{n}}$ is the normal derivative. In the system, Eqs. (1) and (2) are the Darcy system with time derivative retained for flow in porous medium [4, 33]. $\mathbf{u}$ is the nondimensionalized seepage velocity and p is the non-dimensionalized modified pressure [27]. The Eqs. (3) and (4) are the Cahn-Hilliard equations with ϕ being the non-dimensionalized order parameter/phase field variable (such as the concentration difference) and μ the dimensionless chemical potential. We remark that the dimensionless form of the equations would be different in the Hele-Shaw setting, cf. [27, 28] for details.

The parameters in the CHD system are given as follows. Re is the usual Reynold's number. Da is the Darcy number, a measure of the permeability relative to the area of the domain. χ is the porosity. We^* is the ratio of the modified capillary number and Darcy number (equal to the modified Weber number divided by Reynolds number and Darcy number). ϵ is the Cahn number (a measure of the non-dimensionalized thickness of the transition layer between the two phases). We note that the order parameter ϕ takes values 1 and -1 in the bulk of each pure fluid and varies continuously across the transition layer of thickness ϵ. Pe is the diffusional Peclet number measuring the importance of advection over diffusion. $m(\phi)$ is the dimensionless mobility. Finally, $\alpha(\phi)$ is the reciprocal of the dimensionless hydraulic conductivity $\alpha(\phi) = \frac{\eta(\phi)}{\Pi}$ with $\eta(\phi)$ the dimensionless viscosity coefficient and Π the dimensionless permeability. In the CHD system (1)–(6), the densities of the two fluids are assumed to be matched. In this manuscript, we also treat the case where the densities of the binary fluids differ slightly so that the Boussinesq approximation can be applied (cf. [28, 26]). Throughout, we assume $\alpha(\phi)$ and $m(\phi)$ are bounded below and above, i.e.,

$$0 < \alpha_1 \le \alpha(\phi) \le \alpha_2, \quad 0 < m_1 \le m(\phi) \le m_2. \tag{7}$$

Note that the Reynolds number Re and Darcy number Da are typically small for flow in porous medium. Formally setting $Da = 0$ in Eq. (1), one would recover the standard Cahn-Hilliard-Hele-Shaw/Darcy system that has been studied by many authors [27, 28, 42, 10, 41, 40, 29, 23, 17]. The current version of the CHD model is heuristically more accurate as the transient effect of the flow has been taken into account, cf. [18, 5].

An important feature of the CHD system is that it satisfies an energy law. Introduce the total energy

$$E = ReDa \int_\Omega \frac{1}{2\chi}|\mathbf{u}|^2\,dx + \frac{1}{We^*}\int_\Omega \chi\big[\frac{1}{\epsilon}F(\phi) + \frac{\epsilon}{2}|\nabla\phi|^2\big]\,dx. \tag{8}$$

where the first integral represents the total kinetic energy, and the second one is the total free energy of the system with a double-well potential $F(\phi) = \frac{1}{4}(\phi^2-1)^2$. It is clear that the CHD system is energy dissipative

$$\frac{dE}{dt} = -\frac{\epsilon^{-1}}{We^*Pe}\int_\Omega m(\phi)|\nabla\mu|^2\,dx - \int_\Omega \alpha(\phi)|\mathbf{u}|^2\,dx \le 0. \tag{9}$$

The aim of this work is to design an efficient, high order accurate numerical algorithm for solving the CHD system which satisfies a modified discrete energy law mimicking (9). We note that the CHD system is a high order, strongly coupled, nonlinear system that describes physical phenomena of steep spatial variation within a small transition region [2, 30, 31]. It is essential for the numerical scheme to be unconditionally stable so that the numerical stiffness can be handled with ease. There are many coupled, first order accurate numerical schemes which satisfy discrete analogues of the energy law (thus unconditionally stable) for solving diffuse interface models such as the CHD system. See for instance, [42, 10, 15] for Cahn-Hilliard-Darcy case, [6] for Cahn-Hilliard-Stokes case, and [9, 24, 36, 34, 11, 16] for Cahn-Hilliard-Navier-Stokes system. In these schemes, typically a nonlinear unconditionally stable solver (such as convex-splitting schemes [8]) is applied in solving the Cahn-Hilliard Eqs. (3) and (4). To ensure the overall energy-law preservation, they all treat the velocity in the Eq. (3) implicitly. Hence a large nonlinear coupled system has to be solved at every time step.

In recent years, decoupled first order accurate unconditionally stable numerical algorithms have been proposed for solving various types of Cahn-Hilliard fluid models. Notably are the ones proposed in [32, 37, 38] for solving Cahn-Hilliard-Navier-Stokes phase field models. These numerical schemes employ the idea of fractional step method in the update of velocity, in which an intermediate velocity is defined only through the Korteweg forcing term

$\frac{\epsilon^{-1}}{We^*}\phi\nabla\mu$. Thus upon substitution of the intermediate velocity in the Cahn-Hilliard equation, the computation of the Cahn-Hilliard equation is then decoupled from that of fluid equation. In general, nonlinear solvers are only needed for solving the Cahn-Hilliard equation in these schemes. Therefore these decoupled schemes are much more efficient than those coupled ones while maintaining the energy stability. Based on the fractional step method and pressure stabilization technique [14], a decoupled unconditionally stable numerical scheme is recently proposed for solving the standard CHD system [17]. However, the fractional stepping approach in these first order schemes does not seem to have a direct generalization to higher order unconditionally stable schemes, as the splitting error in these methods is only of first order accuracy.

In this paper, we contribute a second order in time, decoupled, unconditionally stable numerical scheme for solving the CHD system (1)-(6). A second order convex splitting method is utilized in the discretization of the nonlinear Cahn-Hilliard equation. Similar convex splitting schemes have been proposed for solving nonlinear equations with gradient flow structure, cf. [22, 3, 35, 19]. Moreover, a second order pressure correction scheme is applied for the time stepping of the Darcy Eqs. (1) and (2). The key point here is that the intermediate velocity is defined through the entire Darcy equation with explicit pressure which is simply an algebraic equation. Thus one not only accomplishes decoupling once substituting the intermediate velocity into Cahn-Hilliard equation but also maintains second order accuracy. As in the case of Cahn-Hilliard-Navier-Stokes system [19], we show that our scheme is uniquely solvable, mass-conservative and satisfies a modified energy law which implies its unconditional stability. We verify the second order accuracy of our scheme via numerical experiments. Finally, we demonstrate the superior performance of our numerical scheme in capturing interfacial topological changes such as interface pinchoff, cf. [28]. The numerical results indicate that our scheme can accurately capture not only the pinchoff of the initial interface but also the subsequent pinchoff of satellite drops, which were produced earlier in [28] using explicit high order methods with very small time-step size. To the best of our knowledge, our scheme is the first decoupled (in order parameter and velocity), second order accurate, unconditionally stable numerical algorithm for solving Cahn-Hilliard fluid models.

There are very few second order schemes for solving phase field fluid models. In [25], a strongly coupled, second-order accurate fully implicit time discretization is proposed for solving the Cahn-Hilliard-Navier-Stokes

system. In the scheme, a non-linear stabilization term is introduced in the Navier-Stokes solver to ensure stability. We recently derived a second order accurate unconditionally stable uniquely solvable numerical scheme for the same Cahn-Hilliard-Navier-Stokes system [19]. However, we only achieved the decoupling of velocity and pressure via pressure correction method. Aiming for a complete decoupling of the system, a linear second order time stepping scheme is designed in [7] for the numerical simulation of the Cahn-Hilliard-Navier-Stokes system with variable density. The scheme is efficient since it involves only constant matrices for all flow variables in the computation. But the scheme seems to be only conditionally stable. Recently, a careful numerical study on the stability of various linearization techniques for decoupling has been carried out in [1].

The rest of the paper is organized as follows. In section 2, we first give the definition of weak formulation for the CHD system. We then motivate our decoupling strategy via a first order scheme. Then we present the second order in time numerical scheme and prove its unconditional stability. Some numerical results are reported in section 3, in which we demonstrate the second order convergence, stability and conservation of mass of our scheme. Finally, the results of a numerical simulation on interface pinchoff are presented and compared with existing work. We conclude the paper with several remarks in

2 The numerical scheme

2.1 The weak formulation

We formulate the CHD system (1)-(6) in a weak form. We introduce the following Hilbert spaces

$$\mathbf{X} = \mathbf{L}^2(\Omega), \quad M = L_0^2(\Omega) = \{q \in L^2(\Omega), \int_\Omega q = 0\}, \tag{10}$$

$$\mathbf{H} = \{\mathbf{v} \in \mathbf{L^2}(\Omega), \nabla \cdot \mathbf{v} = 0, \mathbf{v} \cdot \mathbf{n}|_{\partial\Omega} = 0\}, \tag{11}$$

$$Y = H^1(\Omega). \tag{12}$$

A weak formulation and solutions to the initial-boundary value problem (1)–(6) can be defined similarly as in [10].

Definition 2.1. *Let $\phi_0 \in Y, \mathbf{u}_0 \in \mathbf{H}$. A quadruple $\{\mathbf{u}, p, \phi, \mu\}$ is called a*

weak solution of problem (1)-(6) *if it satisfies*

$$\mathbf{u} \in L^\infty(0,T;\mathbf{H}), \quad \mathbf{u}_t \in L^{\frac{4}{3}}(0,T;\mathbf{H}') \tag{13}$$

$$\phi \in L^\infty(0,T;Y) \cap L^4(0,T;L^\infty(\Omega)), \quad \partial_t\phi \in L^2(0,T;Y'), \tag{14}$$

$$\mu \in L^2(0,T;Y), \quad p \in L^{\frac{4}{3}}(0,T;M), \tag{15}$$

and there hold, $\forall\{\mathbf{v},q,v,\varphi\} \in \mathbf{X}\times M\times Y\times Y$ *and* $t\in(0,T)$ *a.e.*

$$\frac{ReDa}{\chi}\langle\partial_t\mathbf{u},\mathbf{v}\rangle + (\alpha(\phi)\mathbf{u},\mathbf{v}) - (p,\nabla\cdot\mathbf{v}) + \frac{\epsilon^{-1}}{We^*}(\phi\nabla\mu,\mathbf{v}) + (\nabla\cdot\mathbf{u},q) = 0, \tag{16}$$

$$\chi\langle\partial_t\phi,v\rangle - \big(\phi\mathbf{u},\nabla v\big) + \frac{1}{Pe}(M(\phi)\nabla\mu,\nabla v) = 0, \tag{17}$$

$$(\mu,\varphi) - (\phi^3-\phi,\varphi) - \epsilon^2(\nabla\phi,\nabla\varphi) = 0, \tag{18}$$

with initial condition $\mathbf{u}|_{t=0} = \mathbf{u}_0, \phi|_{t=0} = \phi_0$.

The regularity requirements in (13)–(15) are suggested by the energy law Eq. (9). The existence of such a weak solution can be established similarly as [10] (see also [41, 20, 29]).

2.2 Motivation of the decoupling approach

Let N be a positive integer and $0 = t_0 < t_1 < \cdots < t_N = T$ be a uniform partition of $[0,T]$. Denote by $k := t_n - t_{n-1}$, $n = 1,2\ldots N$, the time step-size.

We motivate the design of our second order decoupled scheme through a first order decoupled scheme. The first order decoupled scheme itself is also a new numerical method. Similar to the scheme in [42], a first order in time, coupled and unconditionally stable numerical method for the CHD system is given as follows

$$\frac{ReDa}{\chi}\frac{\mathbf{u}^{n+1}-\mathbf{u}^n}{k} + \alpha(\phi^n)\mathbf{u}^{n+1} + \nabla p^{n+1} + \frac{\epsilon^{-1}}{We^*}\phi^n\nabla\mu^{n+1} = 0, \tag{19}$$

$$\nabla\cdot\mathbf{u}^{n+1} = 0, \tag{20}$$

$$\chi\frac{\phi^{n+1}-\phi^n}{k} + \nabla\cdot(\phi^n\mathbf{u}^{n+1}) - \frac{1}{Pe}\nabla\cdot\big(m(\phi^n)\nabla\mu^{n+1}\big) = 0, \tag{21}$$

$$(\phi^{n+1})^3 - \phi_h^n + \epsilon^2\Delta\phi^{n+1} - \mu^{n+1} = 0, \tag{22}$$

with the boundary conditions

$$\partial_{\mathbf{n}}\phi^{n+1}|_{\partial\Omega} = 0, \quad \partial_{\mathbf{n}}\mu^{n+1}|_{\partial\Omega} = 0, \quad \mathbf{u}^{n+1}\cdot\mathbf{n}|_{\partial\Omega} = 0.$$

We see that the Darcy equations (Eqs. (19) (20)) are coupled with the Cahn-Hilliard system (Eqs. (21) (22)) via the advection velocity $\mathbf{u}^{n+1}$ in Eq. (21). Thanks to the simple structure of the Darcy equation, the velocity $\mathbf{u}^{n+1}$ can be expressed explicitly as a function of ∇p^{n+1} and μ^{n+1}. Thus the coupling is essentially through the implicit discretization of the pressure gradient. In order to decouple the computation of the Darcy system and Cahn-Hilliard system, it is necessary to treat the pressure gradient explicitly and define an intermediate velocity $\overline{\mathbf{u}}^{n+1}$. An extra correction step is then needed to compensate the explicit treatment of the pressure gradient and the resulting loss of divergence-free condition. This is the idea of pressure-correction scheme commonly used for solving the incompressible Navier-Stokes system, cf. [12] and references therein. In this spirit, a first order accurate, decoupled and unconditionally stable numerical scheme is

$$\frac{ReDa}{\chi}\frac{\overline{\mathbf{u}}^{n+1}-\mathbf{u}^{n}}{k}+\alpha(\phi^{n})\overline{\mathbf{u}}^{n+1}+\nabla p^{n}+\frac{\epsilon^{-1}}{We^{*}}\phi^{n}\nabla\mu^{n+1}=0, \tag{23}$$

$$\chi\frac{\phi^{n+1}-\phi^{n}}{k}+\nabla\cdot(\phi^{n}\overline{\mathbf{u}}^{n+1})-\frac{1}{Pe}\nabla\cdot\big(m(\phi^{n})\nabla\mu^{n+1}\big)=0, \tag{24}$$

$$(\phi^{n+1})^{3}-\phi^{n}+\epsilon^{2}\Delta\phi^{n+1}-\mu^{n+1}=0, \tag{25}$$

$$\frac{ReDa}{\chi}\frac{\mathbf{u}^{n+1}-\overline{\mathbf{u}}^{n+1}}{k}+\nabla(p^{n+1}-p^{n})=0,\quad \nabla\cdot\mathbf{u}^{n+1}=0, \tag{26}$$

with boundary conditions

$$\partial_{\mathbf{n}}\phi^{n+1}|_{\partial\Omega}=0,\quad \partial_{\mathbf{n}}\mu^{n+1}|_{\partial\Omega}=0,\quad \mathbf{u}^{n+1}\cdot\mathbf{n}|_{\partial\Omega}=0. \tag{27}$$

We remark how the boundary condition is imposed for the intermediate velocity $\overline{\mathbf{u}}^{n+1}$ in the scheme (19)-(27). Notice that the boundary conditions in Eq. (6) imply $\partial_{\mathbf{n}}p=0$ on the boundary $\partial\Omega$. One can solve for the initial pressure p^{0} via a pressure Poisson equation with the homogeneous Neumann boundary condition. Eq. (23) together with the boundary conditions (27) then imply $\overline{\mathbf{u}}^{n+1}\cdot\mathbf{n}|_{\partial\Omega}=0$. Eq. (26) now yields $\nabla(p^{n+1}-p^{n})\cdot\mathbf{n}|_{\partial\Omega}=0$ which gives $\nabla p^{n+1}\cdot\mathbf{n}=0$. We note also that the intermediate velocity $\overline{\mathbf{u}}^{n+1}$ never appears in actual computation, as it can be simply solved for from Eq. (23). To achieve second order temporal accuracy, one needs to apply a second order pressure correction scheme for the Darcy equation. Following [19], this leads to a second order decoupled unconditionally stable numerical algorithm for solving the CHD system.

2.3 The second order scheme

Here we present our second order in time numerical scheme for solving the CHD system. For convenience, the following notations will be assumed

throughout the paper,

$$\phi^{n+\frac{1}{2}} = \frac{1}{2}(\phi^{n+1} + \phi^n), \quad \widetilde{\phi}^{n+\frac{1}{2}} = \frac{3\phi^n - \phi^{n-1}}{2}, \tag{28a}$$

$$\overline{\mathbf{u}}^{n+\frac{1}{2}} = \frac{\overline{\mathbf{u}}^{n+1} + \mathbf{u}^n}{2}, \quad \mu^{n+\frac{1}{2}} = \frac{1}{2}(\mu^{n+1} + \mu^n). \tag{28b}$$

The semi-discrete (discrete in time, continuous in space) numerical scheme takes the form

$$\frac{ReDa}{\chi}\frac{\overline{\mathbf{u}}^{n+1} - \mathbf{u}^n}{k} + \alpha(\widetilde{\phi}^{n+\frac{1}{2}})\overline{\mathbf{u}}^{n+\frac{1}{2}} + \nabla p^n + \frac{\epsilon^{-1}}{We^*}\widetilde{\phi}^{n+\frac{1}{2}}\nabla\mu^{n+\frac{1}{2}} = 0, \tag{29}$$

$$\chi\frac{\phi^{n+1} - \phi^n}{k} + \nabla\cdot(\widetilde{\phi}^{n+\frac{1}{2}}\overline{\mathbf{u}}^{n+\frac{1}{2}}) - \frac{1}{Pe}\nabla\cdot\big(m(\widetilde{\phi}^{n+\frac{1}{2}})\nabla\mu^{n+\frac{1}{2}}\big) = 0, \tag{30}$$

$$\frac{1}{2}\big((\phi^{n+1})^2 + (\phi^n)^2\big)\phi^{n+\frac{1}{2}} - \widetilde{\phi}^{n+\frac{1}{2}} + \epsilon^2\Delta\phi^{n+\frac{1}{2}} - \mu^{n+\frac{1}{2}} = 0, \tag{31}$$

$$\frac{ReDa}{\chi}\frac{\mathbf{u}^{n+1} - \overline{\mathbf{u}}^{n+1}}{k} + \frac{1}{2}\nabla(p^{n+1} - p^n) = 0, \quad \nabla\cdot\mathbf{u}^{n+1} = 0, \tag{32}$$

with boundary conditions

$$\partial_{\mathbf{n}}\phi^{n+1}|_{\partial\Omega} = 0, \quad \partial_{\mathbf{n}}\mu^{n+1}|_{\partial\Omega} = 0, \quad \mathbf{u}^{n+1}\cdot\mathbf{n}|_{\partial\Omega} = 0. \tag{33}$$

Overall, the scheme can be viewed as a second order Crank-Nicolson time discretization combined with the second order Adams-Bashforth extrapolation. A similar scheme has been proposed to solve the Cahn-Hilliard-Navier-Stokes system [19]. As motivated in the previous subsection, Eqs. (29) and (32) are derived from a second order pressure correction scheme due to van Kan [39] applied to the Darcy system. The splitting error is formally of second order, as Eq. (32) can be interpreted as

$$\mathbf{u}^{n+1} = \overline{\mathbf{u}}^{n+1} - k\frac{\chi}{2ReDa}\nabla(p^{n+1} - p^n) \approx \overline{\mathbf{u}}^{n+1} - k^2\frac{\chi}{2ReDa}\nabla p_t|_{t=t_{n+\frac{1}{2}}}.$$

Adding Eqs. (29) and (32) together gives

$$\frac{ReDa}{\chi}\frac{\mathbf{u}^{n+1} - \mathbf{u}^n}{k} + \alpha(\widetilde{\phi}^{n+\frac{1}{2}})\overline{\mathbf{u}}^{n+\frac{1}{2}} + \nabla\frac{p^{n+1} + p^n}{2} + \frac{\epsilon^{-1}}{We^*}\widetilde{\phi}^{n+\frac{1}{2}}\nabla\mu^{n+\frac{1}{2}} = 0,$$
$$\nabla\cdot\mathbf{u}^{n+1} = 0,$$

which is a second order approximation of the Darcy system.

The first two terms in Eq. (31), i.e. $\frac{1}{2}\big((\phi^{n+1})^2 + (\phi^n)^2\big)\phi^{n+\frac{1}{2}} - \widetilde{\phi}^{n+\frac{1}{2}}$, comprise a second order approximation of $\phi^3 - \phi$. They are derived according to the idea of convex-splitting of the corresponding energy density function

$F(\phi) = \frac{1}{4}(\phi^2-1)^2$. Note that $\phi^3 - \phi = F'(\phi)$. We write $F(\phi)$ as the sum of a convex function and a concave function

$$F(\phi) = F_v(\phi) + F_c(\phi) := \frac{1}{4}\phi^4 + \big(-\frac{1}{2}\phi^2 + \frac{1}{4}\big),$$

and accordingly $F'(\phi) = F_v'(\phi) + F_c'(\phi)$. We then treat the convex part implicitly (i.e., $F_v'(\phi^{k+\frac{1}{2}})$) and the concave part explicitly (i.e. $F_c'(\widetilde{\phi}^{n+\frac{1}{2}})$). We approximate $F_v'(\phi^{k+\frac{1}{2}})$ further by the Crank-Nicolson scheme

$$F_v'(\phi^{k+\frac{1}{2}}) \approx \frac{f_v(\phi^{k+1}) - f_v(\phi^k)}{\phi^{k+1}-\phi^k} = \frac{1}{2}[(\phi^{k+1})^2 + (\phi^k)^2]\phi^{k+\frac{1}{2}}.$$

First order convex-splitting schemes are well known for solving equations with gradient flow structure, cf. [8, 42] and references therein. Recently, second order convex-splitting schemes have been proposed in various contexts [22, 3, 35, 19].

Finally, we comment on how to implement the scheme (29)-(33). We notice that $\overline{\mathbf{u}}^{n+\frac{1}{2}}$ or the equivalent $\overline{\mathbf{u}}^{n+1}$ can be found explicitly from Eq. (29). After substitution into Eqs. (30) and (32), we see that the intermediate velocity never appears in the real computation. Indeed, the system (29)-(33) can be effectively written as

$$\chi\frac{\phi^{n+1}-\phi^n}{k} + \nabla\cdot\big(\widetilde{\phi}^{n+\frac{1}{2}}[\beta_1(\widetilde{\phi}^{n+\frac{1}{2}})\mathbf{u}^n - \beta_2(\widetilde{\phi}^{n+\frac{1}{2}})\nabla p^n]\big) - \nabla\cdot\big(\overline{m}(\widetilde{\phi}^{n+\frac{1}{2}})\nabla\mu^{n+\frac{1}{2}}\big) = 0, \tag{34}$$

$$\frac{1}{2}\big((\phi^{n+1})^2 + (\phi^n)^2\big)\phi^{n+\frac{1}{2}} - \widetilde{\phi}^{n+\frac{1}{2}} + \epsilon^2\Delta\phi^{n+\frac{1}{2}} - \mu^{n+\frac{1}{2}} = 0, \tag{35}$$

$$\frac{ReDa}{\chi k}\Big[\mathbf{u}^{n+1} - \big(\beta_1(\widetilde{\phi}^{n+\frac{1}{2}}) - \alpha(\widetilde{\phi}^{n+\frac{1}{2}})\beta_2(\widetilde{\phi}^{n+\frac{1}{2}})\big)\mathbf{u}^n + 2\beta_2(\widetilde{\phi}^{n+\frac{1}{2}})\big(\nabla p^n + \frac{\epsilon^{-1}}{We^*}\widetilde{\phi}^{n+\frac{1}{2}}\nabla\mu^{n+\frac{1}{2}}\big)\Big] \tag{36}$$

$$+\frac{1}{2}\nabla(p^{n+1}-p^n) = 0,$$

$$\nabla\cdot\mathbf{u}^{n+1} = 0, \tag{37}$$

with boundary conditions

$$\partial_{\mathbf{n}}\phi^{n+1}|_{\partial\Omega} = 0, \quad \partial_{\mathbf{n}}\mu^{n+1}|_{\partial\Omega} = 0, \quad \mathbf{u}^{n+1}\cdot\mathbf{n}|_{\partial\Omega} = 0. \tag{38}$$

Here the functions β_1, β_2 and $\overline{m}$ are defined as follows

$$\beta_1(\widetilde{\phi}^{n+\frac{1}{2}}) = \frac{2ReDa}{2ReDa + \alpha(\widetilde{\phi}^{n+\frac{1}{2}})k\chi},$$

$$\beta_2(\widetilde{\phi}^{n+\frac{1}{2}}) = \frac{k\chi}{2ReDa + \alpha(\widetilde{\phi}^{n+\frac{1}{2}})k\chi},$$

$$\overline{m}(\widetilde{\phi}^{n+\frac{1}{2}}) = \frac{m(\widetilde{\phi}^{n+\frac{1}{2}})}{Pe} + \beta_2\frac{\epsilon^{-1}}{We^*}(\widetilde{\phi}^{n+\frac{1}{2}})^2.$$

Hence the Cahn-Hilliard system is completely decoupled from the Darcy system, which yields a very efficient solver for the CHD equations. We note that the Eq. (36) can be written as, after some lengthy algebra

$$\frac{ReDa}{\chi}\frac{\mathbf{u}^{n+1}-\mathbf{u}^n}{k}+\alpha(\widetilde{\phi}^{n+\frac{1}{2}})\frac{\mathbf{u}^{n+1}+\mathbf{u}^n}{2}+\frac{1}{2}\nabla(p^{n+1}+p^n) \tag{39}$$
$$+\frac{\epsilon^{-1}}{We^*}\widetilde{\phi}^{n+\frac{1}{2}}\nabla\mu^{n+\frac{1}{2}}+\frac{\alpha(\widetilde{\phi}^{n+\frac{1}{2}})\chi}{4ReDa}k\nabla(p^{n+1}-p^n)=0.$$

It is clear that Eq. (39) is a second order in time approximation of the PDE (1). In the next subsection, we show that the scheme is unconditionally stable.

2.4 Stability of the second order scheme

Following [19], we show that the second order scheme (29)-(33) satisfies a modified energy law and is unconditionally stable. We define a discrete energy functional at time level t_n as

$$E^n := ReDa\int_\Omega\frac{1}{2\chi}|\mathbf{u}^n|^2\,dx+\frac{1}{We^*}\int_\Omega\chi\big[\frac{1}{\epsilon}F(\phi^n)+\frac{\epsilon}{2}|\nabla\phi^n|^2\big]\,dx.$$

For the scheme (29)-(33), the following theorem is valid.

Theorem 2.1. *Given $\phi^n,\mathbf{u}^n,p^n$ such that*

$$\partial_{\mathbf{n}}\phi^n|_{\partial\Omega}=0,\quad \partial_{\mathbf{n}}p^n|_{\partial\Omega}=0,\quad \mathbf{u}^n\cdot\mathbf{n}|_{\partial\Omega}=0, \tag{40}$$

there exists a unique solution $\{\phi^{n+1},\mu^{n+\frac{1}{2}},\mathbf{u}^{n+1},p^{n+1}\}$ to the scheme (29)–(33) at each time step. In addition, the scheme is mass-conservative in the sense

$$\int_\Omega\phi^{n+1}=\int_\Omega\phi^n,\quad n=0,1,\cdots,N-1. \tag{41}$$

Moreover, the solution satisfies a modified energy law

$$\Big\{E^{n+1}+\frac{\epsilon^{-1}}{4We^*}||\phi^{n+1}-\phi^n||_{L^2}^2+\frac{\chi}{ReDa}\frac{k^2}{8}||\nabla p^{n+1}||_{L^2}^2\Big\} \tag{42}$$
$$-\Big\{E^n+\frac{\epsilon^{-1}}{4We^*}||\phi^n-\phi^{n-1}||_{L^2}^2+\frac{\chi}{ReDa}\frac{k^2}{8}||\nabla p^n||_{L^2}^2\Big\}$$
$$\le -k\frac{\epsilon^{-1}}{PeWe^*}||\sqrt{m}\nabla\mu^{n+\frac{1}{2}}||_{L^2}^2-k||\sqrt{\alpha}\overline{\mathbf{u}}^{n+\frac{1}{2}}||_{L^2}^2-\frac{\chi\epsilon^{-1}}{4We^*}||\phi^{n+1}-2\phi^n+\phi^{n-1}||_{L^2}^2.$$

Thus, the scheme is unconditionally energy stable.

Proof. The unique solvability of Eqs. (29)–(33) (or equivalent (34)–(38)) can be established easily thanks to the decoupling and the convex-splitting treatment of the chemical potential equation. Here we omit the details of the proof but point to the appropriate references. Given $\widetilde{\phi}^{n+\frac{1}{2}}, \mathbf{u}^n$ and p^n, Eqs. (34) and (35) amount to a second-order convex-splitting discretization of the Cahn-Hilliard equation with known source terms. Thus the unique solvability of the Cahn-Hilliard part follows from a variational argument by exploiting the convexity in the design and the gradient flow structure of the system, cf. [34] for a similar argument for the Allen-Cahn case (see also [24, 42]). Once $\mu^{n+\frac{1}{2}}$ is known, Eqs. (36)–(37) are the linear Darcy system with forcing terms. We note that the unique solvability can also be established via a monotonicity argument, cf. [19, 20] for details.

For the mass-conservation (41), one simply integrates Eq. (34), performs integration by parts and utilizes the boundary conditions (38) and (40).

We now show that the scheme is unconditionally stable. Notice that the boundary conditions (38) and (40) imply $\overline{\mathbf{u}}^{n+\frac{1}{2}} \cdot \mathbf{n}\big|_{\partial\Omega} = 0$. One first takes the L^2 inner product of Eq. (29) with $k\mu^{k+\frac{1}{2}}$ to obtain

$$\chi\big(\phi^{n+1} - \phi^n, \mu^{n+\frac{1}{2}}\big) = -\frac{k}{Pe}||\sqrt{m}\nabla\mu^{n+\frac{1}{2}}||_{L^2}^2 + k\big(\widetilde{\phi}^{n+\frac{1}{2}}\overline{\mathbf{u}}^{n+\frac{1}{2}}, \nabla\mu^{n+\frac{1}{2}}\big). \tag{43}$$

Next, multiplying Eq. (30) by $(\phi^{n+1} - \phi^n)$, performing integration by parts and using the the following identity

$$\begin{aligned}
& \big(\widetilde{\phi}^{n+\frac{1}{2}}, \phi^{n+1} - \phi^n\big) \\
= \;& \frac{1}{2}\big(3\phi^n - \phi^{n-1}, \phi^{n+1} - \phi^n\big) \\
= \;& \frac{1}{2}\big(\phi^{n+1} + \phi^n, \phi^{n+1} - \phi^n\big) - \frac{1}{2}\big(\phi^{n+1} - 2\phi^n + \phi^{n-1}, \phi^{n+1} - \phi^n\big) \\
= \;& \frac{1}{2}\big(||\phi^{n+1}||_{L^2}^2 - ||\phi^n||_{L^2}^2\big) - \frac{1}{4}\{||\phi^{n+1} - \phi^n||_{L^2}^2 - ||\phi^n - \phi^{n-1}||_{L^2}^2 \\
& + ||\phi^{n+1} - 2\phi^n + \phi^{n-1}||_{L^2}^2\},
\end{aligned}$$

one deduces

$$\begin{aligned}
& -\big(\phi^{n+1} - \phi^n, \mu^{n+\frac{1}{2}}\big) + \big(F(\phi^{n+1}) - F(\phi^n), 1\big) + \frac{\epsilon^2}{2}(||\nabla\phi^{n+1}||_{L^2}^2 - ||\nabla\phi^n||_{L^2}^2) \\
& + \frac{1}{4}\{||\phi^{n+1} - \phi^n||_{L^2}^2 - ||\phi^n - \phi^{n-1}||_{L^2}^2 + ||\phi^{n+1} - 2\phi^n + \phi^{n-1}||_{L^2}^2\} = 0,
\end{aligned} \tag{44}$$

where one has utilized the definition of $F(\phi) = \frac{1}{4}(\phi^2 - 1)^2$. Multiplying (44)

with χ and adding the result to Eq. (43) gives

$$\chi\Big\{\big(F(\phi^{n+1})-F(\phi^n),1\big)+\frac{\epsilon^2}{2}(||\nabla\phi^{n+1}||_{L^2}^2-||\nabla\phi^n||_{L^2}^2)+\frac{1}{4}(||\phi^{n+1}-\phi^n||_{L^2}^2-||\phi^n-\phi^{n-1}||_{L^2}^2)\Big\} \tag{45}$$

$$=-\frac{\chi}{4}||\phi^{n+1}-2\phi^n+\phi^{n-1}||_{L^2}^2-\frac{k}{Pe}||\sqrt{m}\nabla\mu^{n+\frac{1}{2}}||_{L^2}^2+k\big(\widetilde{\phi}^{n+\frac{1}{2}}\overline{\mathbf{u}}^{n+\frac{1}{2}},\nabla\mu^{n+\frac{1}{2}}\big).$$

Next, taking the L^2 inner product of Eq. (29) with $k\overline{\mathbf{u}}^{n+\frac{1}{2}}$, one obtains

$$\frac{ReDa}{2\chi}(||\overline{\mathbf{u}}^{n+1}||_{L^2}^2-||\mathbf{u}^n||_{L^2}^2)+k||\sqrt{\alpha}\overline{\mathbf{u}}^{n+\frac{1}{2}}||_{L^2}^2=-k\big(\nabla p^n,\overline{\mathbf{u}}^{n+\frac{1}{2}}\big)-k\frac{\epsilon^{-1}}{We^*}\big(\widetilde{\phi}^{n+\frac{1}{2}}\nabla\mu^{n+\frac{1}{2}},\overline{\mathbf{u}}^{n+\frac{1}{2}}\big). \tag{46}$$

Testing the first equation in (32) by $\mathbf{u}^{n+1}k$ and performing integration by parts yield

$$\frac{ReDa}{2\chi}(||\mathbf{u}^{n+1}||_{L^2}^2-||\overline{\mathbf{u}}^{n+1}||_{L^2}^2+||\mathbf{u}^{n+1}-\overline{\mathbf{u}}^{n+1}||_{L^2}^2)=0, \tag{47}$$

where one has utilized explicitly the divergence-free condition

$$\big(\nabla(p^{n+1}-p^n),\mathbf{u}^{n+1}\big)=-\big((p^{n+1}-p^n),\nabla\cdot\mathbf{u}^{n+1}\big)=0.$$

Next, we rewrite the projection step Eq. (32) as

$$\frac{ReDa}{\chi}\frac{\mathbf{u}^{n+1}+\mathbf{u}^n-2\overline{\mathbf{u}}^{n+\frac{1}{2}}}{k}+\frac{1}{2}\nabla(p^{n+1}-p^n)=0.$$

Testing the above equation with $\frac{k^2}{2}\nabla p^n$, one arrives at

$$\frac{k^2}{8}\big\{||\nabla p^{n+1}||_{L^2}^2-||\nabla p^n||_{L^2}^2-||\nabla(p^{n+1}-p^n)||_{L^2}^2\big\}=k\frac{ReDa}{\chi}\big(\nabla p^n,\overline{\mathbf{u}}^{n+\frac{1}{2}}\big). \tag{48}$$

On the other hand, one obtains, by testing Eq. (32) with $\nabla(p^{n+1}-p^n)$ and applying the Cauchy-Schwarz inequality,

$$\frac{k^2}{8}||\nabla(p^{n+1}-p^n)||_{L^2}^2\le\big(\frac{ReDa}{\chi}\big)^2\frac{1}{2}||\mathbf{u}^{n+1}-\overline{\mathbf{u}}^{n+1}||_{L^2}^2.$$

Eq. (48) then becomes

$$\frac{\chi}{ReDa}\frac{k^2}{8}\big\{||\nabla p^{n+1}||_{L^2}^2-||\nabla p^n||_{L^2}^2\big\}-\frac{ReDa}{2\chi}||\mathbf{u}^{n+1}-\overline{\mathbf{u}}^{n+1}||_{L^2}^2\le k\big(\nabla p^n,\overline{\mathbf{u}}^{n+\frac{1}{2}}\big). \tag{49}$$

Now summing up Eqs. (46), (47) and (49), one obtains

$$\frac{ReDa}{2\chi}(||\mathbf{u}^{n+1}||_{L^2}^2 - ||\mathbf{u}^n||_{L^2}^2) + \frac{\chi}{ReDa}\frac{k^2}{8}\{||\nabla p^{n+1}||_{L^2}^2 - ||\nabla p^n||_{L^2}^2\} \quad (50)$$
$$\leq -k||\sqrt{\alpha}\overline{\mathbf{u}}^{n+\frac{1}{2}}||_{L^2}^2 - k\frac{\epsilon^{-1}}{We^*}(\widetilde{\phi}^{n+\frac{1}{2}}\nabla\mu^{n+\frac{1}{2}}, \overline{\mathbf{u}}^{n+\frac{1}{2}}).$$

The energy law (42) then follows from summing up the multiple of Eq. (45) by $\frac{\epsilon^{-1}}{We^*}$ and Eq. (50).

□

The scheme (29)–(33) (or equivalent (34)–(38)) can be further discretized in space by common spatial discretization methods such as spectral methods, finite element or finite difference methods. The unconditional stability of the fully discrete numerical schemes are expected to hold as well. In the appendix, we give a fully discrete formulation based on the finite element method which inherits the same unconditional stability from the semi-discrete scheme, as long as one chooses appropriate finite element spaces for velocity and pressure. We defer the error analysis of such fully discrete schemes to a future work.

3 Numerical Experiments

In this section, we report some numerical results to show the accuracy and efficiency of the numerical scheme (29)-(33). The scheme is further discretized in space by finite element method. We solve the nonlinear equations (34)-(35) by the classical Newton's method. All the numerical tests are performed using the free software FreeFem++ [21].

3.1 Convergence, stability and conservation of mass

As a first numerical test, we verify that the scheme (29)-(33) is second order accurate in time. For simplicity, all the parameters in the CHD system (1)–(4) are assumed to be unity and the domain is the unit square $\Omega = [0,1]\times[0,1]$. We proceed by the method of manufactured solutions, assuming forcing terms are present in Eqns. (1), (3) and (4) such that the exact

solutions of the system are

$$\mathbf{u} = \Big(-\sin^2(\pi x)\sin(2\pi y)\cos(t), \sin^2(\pi y)\sin(2\pi x)\cos(t)\Big),$$
$$p = \cos(t)(xy - \frac{1}{4}),$$
$$\phi = \cos(t)\cos(\pi x)\cos(\pi y),$$
$$\mu = \sin(t)cos(\pi x)\cos(\pi y).$$

We use P2–P2 finite elements for ϕ_h^{n+1} and μ_h^{n+1}, and Taylor-Hood P2–P1 pair for $\mathbf{u}_h^{n+1}$ and p_h^{n+1}. A linear relation between the spatial resolution and temporal resolution is assumed such that the temporal error is dominant in the following calculation. We successively decrease the time step-size k and compute the error measured in L^2 norm at a final time $T = 0.5$. An error estimate of the form $\mathcal{O}(k^2)$ is anticipated for all the variables, i.e., $\mathbf{u}, \phi, \mu$ and p. The log-log plot of the errors is shown in Fig.1, which clearly demonstrates the second order convergence in time for all variables.

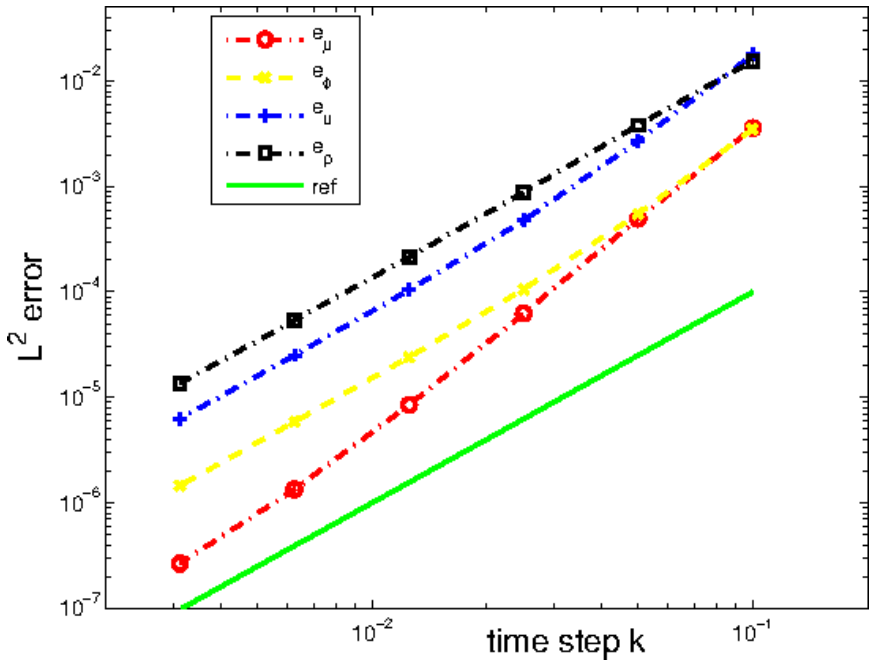

Figure 1: Log-Log plot of the error in L^2 norm for $\mathbf{u}$, p, ϕ and μ as a function of time step k. The solid green line is the reference line $e = 0.01k^2$. The final time is $T = 0.5$. $h = 1.4k$. P2–P2 is used for ϕ and μ, P2–P1 is used for $\mathbf{u}$ and p. The other parameters are set to be unity.

Next, we demonstrate the unconditional stability of the scheme (29)-(33) via the numerical simulation of the spinodal decomposition of a binary fluid.

The set-up of the test is as follows: a well-mixed binary fluid is initially at rest, i.e. $\mathbf{u}_0 = 0$ and $\phi_0 = \bar{\phi} + r(x, y)$ with an average composition $\bar{\phi} = -0.05$ and random $r \in [-0.05, 0.05]$; As the average composition of the phase field variable falls into the so-called unstable spinodal region, the different fluid components quickly separate from each other; Afterwards, the slow process of coarsening dominates. The whole process is energy-dissipative. The stability of the numerical scheme can be examined through the evolution of the discrete energy.

The parameters are $\epsilon = 0.01$, $We^* = 100$, $Pe = 100$, $M(\phi) = \sqrt{(1-\phi^2)^2 + \epsilon^2}$, $\chi = 0.5$, $\frac{ReDa}{\chi} = 0.1$, $\alpha(\phi) = 2$. We take $k = 0.1$ and $h = \frac{\sqrt{2}}{100}$. The discrete energy functional at time level t_n is defined as

$$E^n := ReDa \int_\Omega \frac{1}{2\chi} |\mathbf{u}_h^n|^2 \, dx + \frac{1}{We^*} \int_\Omega \chi \big[\frac{1}{\epsilon} F(\phi_h^n) + \frac{\epsilon}{2} |\nabla \phi_h^n|^2 \big] \, dx.$$

The evolution of this energy functional is shown in Fig. 2.

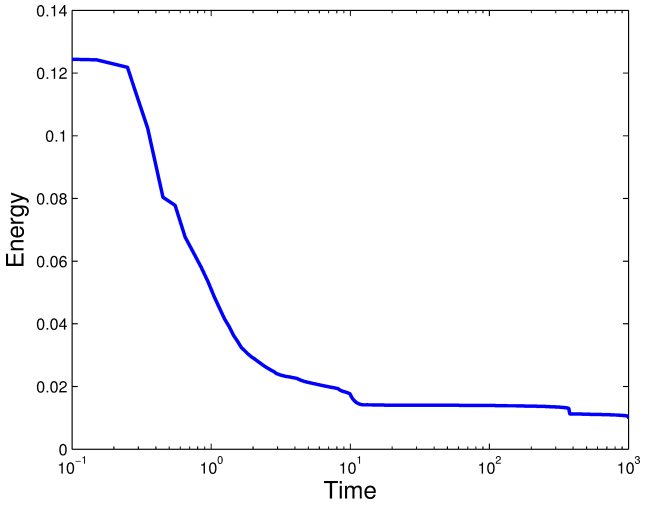

Figure 2: Evolution of the discrete energy in the test of spinodal decomposition. $k = 0.1$ and $h = \frac{\sqrt{2}}{100}$.

In addition, we show the time evolution of the discrete mass $\int_\Omega \phi_h^n dx$ associated with numerical simulation of spinodal decomposition in Fig. 3. Note that $\int_\Omega \phi_0 dx = -0.05$. After projection into the finite element space P1, we have $\int_\Omega \phi_h^0 dx = -0.0499$. Fig. 3 shows that the exact value is preserved throughout the numerical simulation.

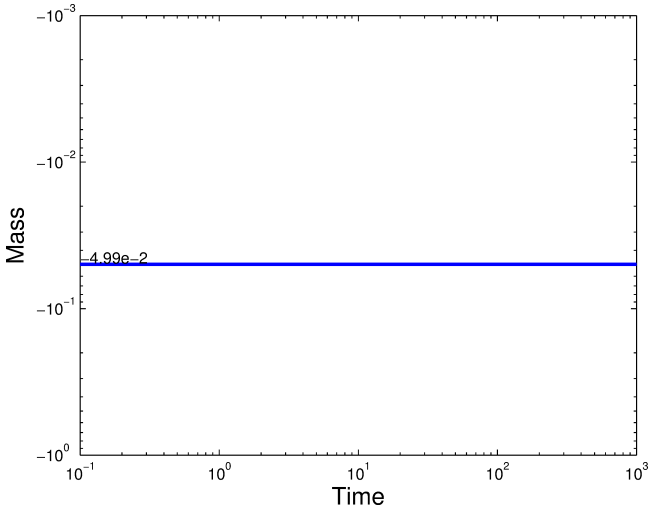

Figure 3: Time evolution of the discrete mass $\int_\Omega \phi_h^n dx$ in the test of spinodal decomposition. $k = 0.1$ and $h = \frac{\sqrt{2}}{100}$.

3.2 Interface pinchoff

One of the main advantages of the diffuse interface models in comparison to the sharp interface models is that they allow for topological changes of the diffuse interface such as interface pinchoff or reconnection. In this numerical experiment, we consider a situation where a light fluid layer is sandwiched by two heavy fluid layers, cf. the diagram 4. Due to boyancy, the lighter fluids rise and the heavier fluid layer on the top eventually penetrates the lighter fluid layer, causing the pinchoff of the fluid interface. This numerical example is first considered by Lee, Lowengrub and Goodman [28] in a Hele-Shaw setting. They investigate carefully the pinchoff event and effects of different parameter values. To obtain accurate approximations, they employ a third order accurate, equilibrium preserving version of a linear propagator in time, and the Fourier pseudospectral methods in space by assuming periodic boundary conditions. See [28] for details. Here we show that the numerical results generated by our numerical algorithm agree well with those reported in [28].

We consider a square domain $\Omega = [0, 2\pi] \times [0, 2\pi]$. The density difference is assumed to be small so that the Boussinesq approximation can be applied (so-called BHSCH system in [28]). More precisely, the background density is chosen as unity and the influence of the density difference is only appreciable in a buoyancy term $-\lambda(\phi - \bar{\phi})\hat{\mathbf{y}}$ on the right-hand side of the Darcy equation (1). Here $\hat{\mathbf{y}}$ is the unit vector pointing upwards ($\hat{\mathbf{y}} = (0, 1)$), $\bar{\phi}$ is the spatially

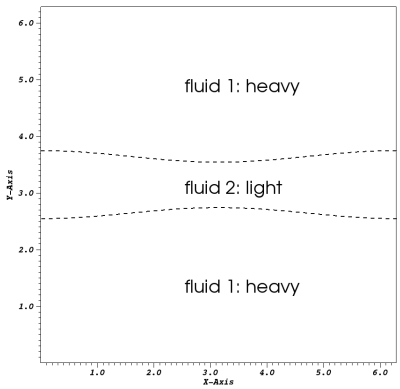

Figure 4: The initial configuration of the binary fluids in the experiment of interface pinchoff. $\epsilon = 0.05$. The dash lines are the zero contour of the interfaces.

averaged order parameter (a constant), and λ is a dimensionless parameter defined as $\lambda = \frac{G(\rho_1-\rho_2)}{2}\frac{\Pi_0}{\eta_0 U_0}$ with G the gravitational constant, Π_0 the scale of permeability, η_0 the scale of viscosity, U_0 the scale of velocity (cf. Eq. (2.16) [26]). We recall the definition of the Bond number B and the Atwood number A, cf. [28],

$$B = \frac{G(\rho_1 - \rho_2)}{\tau}, \qquad A = \frac{\eta_1 - \eta_2}{\eta_1 + \eta_2}, \tag{51}$$

where τ is the surface tension parameter. The initial condition for the phase field variable is defined as

$$\phi_0 = \tanh\big(\frac{y - y_1(x)}{\sqrt{2}\epsilon}\big)\tanh\big(\frac{y - y_2(x)}{\sqrt{2}\epsilon}\big),$$

with

$$y_1(x) = \pi - (0.5 + 0.1\cos(x)), \quad y_2(x) = \pi + (0.5 + 0.1\cos(x)).$$

See Fig. 4 for an illustration of the initial order parameter. In our simulation, boundary conditions (6) are imposed. We remark that periodic boundary conditions are used in [28] by superimposing more fluid layers.

In the simulation, we take $\epsilon = 0.05$, $Pe = 20$, $We^* = 4$, $m(\phi) = 1.0$, , $\chi = 0.5$ and $\frac{ReDa}{\chi} = 0.01$. We will vary λ and $\alpha(\phi)$ in different situations, which will give different values for the Bond number B and Atwood number A defined in (51) [28]. The temporal resolution is fixed at $k = 0.01$. We note that smaller time stepsize $k = 10^{-3}$ has been used in [28] and [17]. In

space, P2–P1 finite elements are used for $\mathbf{u}$ and p, and P2–P2 finite elements are used for ϕ and μ. To resolve the smallness of the diffuse interface, adaptive mesh refinement is carried out every a few time steps according to the Hessian of the order parameter such that approximately 10 grid cells are located across the diffuse interface, cf. [21].

In Fig. 5, we show the evolution of the zero contours of the order parameter $\phi = 0.0$ under different values of λ (giving different Bond numbers B in [28]). The left-most column shows the evolution sequence with $\lambda = 1.18$ ($|B| \approx 10$), the middle column is for $\lambda = 1.89$ ($|B| \approx 16$), and the right-most column corresponds to $\lambda = 2.36$ ($|B| \approx 20$). The viscosity of the two fluids is assumed to be matched $\alpha(\phi) = 1.5$. All other parameters are the same for three simulations. As observed, increasing λ (the buoyancy strength) speeds up the evolution and increases the number of satellite drops after pinchoff. Only one drop is produced when $\lambda = 1.18$ in the first column, while two and three satellite drops are produced via a secondary interface pinchoff when $\lambda = 1.89$ and $\lambda = 2.36$ respectively. Our results are consistent with those reported in [28] (Fig. 16) which were produced using explicit high order numerical methods with very small time-step size. We also remark that the satellite drops after initial pinchoff are not captured by those first order schemes, see for instance [17].

We also consider the cases where the viscosities of the two fluids are different. The mismatched viscosity can introduce an extra instability with the more viscous fluid displaced by less viscous fluid. For simplicity, we choose a linear viscosity function $\alpha(\phi) = \eta_1 \frac{1+\phi}{2} + \eta_2 \frac{1-\phi}{2}$ such that the fluid in the middle layer has viscosity η_2 and the rest of the fluid has viscosity η_1. Fig. 6 shows the evolution of the zero contour of the order parameter where the viscosity configuration may (right column) or may not (left column) induce the extra instability. In the left column, $\eta_1 = 1.5, \eta_2 = 6.0$. Thus there is no instability due to viscosity variation for the upper interface. One observes that there is only one pinchoff event with no satellite drops. In the right column, $\eta_1 = 6.0, \eta_2 = 1.5$ which induces an extra instability in the upper fluid interface. One sees that there is a subsequent pinchoff with two satellite drops produced. This phenomenon is also observed in Fig. 18 of [28].

4 Conclusion

In this paper, we propose a second order in time, fully decoupled, unconditionally stable and mass-conservative numerical scheme for solving the

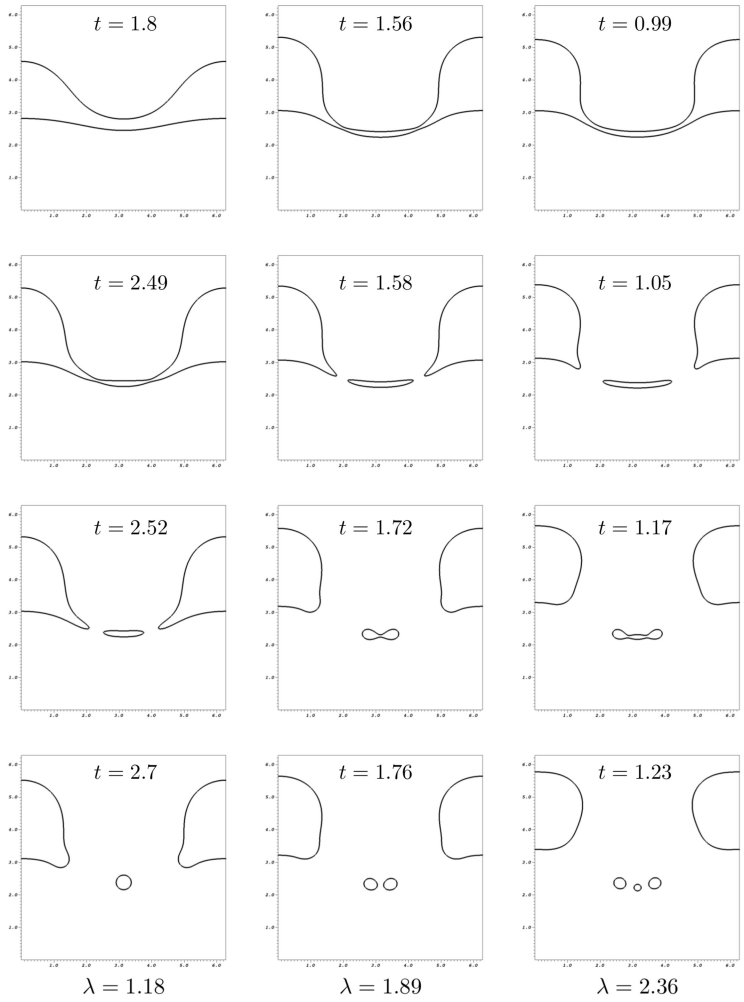

Figure 5: Zero contour plots of the order parameter with matched viscosity. Left-most column, $\lambda = 1.18$; Center column, $\lambda = 1.89$; Right-most column $\lambda = 2.36$. $\epsilon = 0.05$, $\alpha(\phi) = 1.5$, $k = 0.01$.

Cahn-Hilliard-Darcy system modelling two-phase incompressible flows in porous medium or a Hele-Shaw cell. The Cahn-Hilliard equation are solved by a second order convex splitting scheme. A second order pressure correction type method is applied to solve the Darcy equation, which allows for the decoupling of the Cahn-Hilliard solver and the update of the Darcy equation upon substitution of the intermediate velocity, thanks to the algebraic simplicity of the Darcy equation. The scheme is shown to satisfy a modified energy law and is unconditionally energy stable. We show numerically the second order convergence as well as the unconditional stability of the

scheme. Finally, we demonstrate the superior performance of our numerical scheme on the simulation of interface pinchoff. The numerical results show that our scheme can accurately capture not only the pinchoff of the initial interface but also the subsequent pinchoff of satellite drops, which agree well with those in [28] created by explicit high order methods with very small time-step size.

High order, unconditionally stable, decoupled numerical schemes are very desirable for solving diffuse interface models. The key to achieve the decoupling in our scheme is that the intermediate velocity employed in the Cahn-Hilliard equation is governed by a simple algebraic equation. We remark that this simple structure is not present in the scheme for Cahn-Hilliard-Navier-Stokes case, cf. [19]. The generalization of our methodology to other phase field models such as Cahn-Hilliard-Navier-Stokes equation of matched or mismatched densities requires further investigation.

Acknowledgement

This work is supported in part by a grant from the NSF (DMS1312701), and a multidisciplinary support grant from the Florida State University. The authors wish to thank Wenbin Chen, Mike Jolly and Jie Shen for helpful discussions.

Appendix

In this appendix, we give a finite element formulation of the scheme (29)–(33), equivalently, (34)–(38), and prove its unconditional stability. Let $\mathcal{T}_h$ be a regular, quasi-uniform triangulation of the domain Ω in 2D with mesh size h. We introduce a continuous finite element approximation Y_h of the Hilbert space $H^1(\Omega)$ based on $\mathcal{T}_h$. For instance, Y_h can be

$$Y_h = \{v_h \in C(\bar{\Omega}) \big| v_h|_K \in P_r(K), \forall K \in \mathcal{T}_h\},$$

where $P_r(K)$ is the space of polynomials of degree less than or equal to r on the triangle K. We define another space $M_h := Y_h \cap L_0^2(\Omega)$ where L_0^2 is a subspace of L^2 whose elements have zero mean. Finally, we introduce a vector finite element space $\mathbf{X}_h$ which is an approximation of the space $\mathbf{X} = \mathbf{L}^2(\Omega)$. We assume that the spaces M_h and $\mathbf{X}_h$ are compatible in the sense that $\nabla Y_h \subset \mathbf{X}_h$. For instance, if the space Y_h consists of piece-wise continuous polynomials of order less than or equal to r, the vector space $\mathbf{X}_h$

can be chosen as the space of piece-wise polynomials of order less than or equal to $r-1$ (discontinuous).

Then a finite element formulation of the scheme (34)–(38) reads: find $\phi_h^{n+1} \in Y_h$, $\mu_h^{n+\frac{1}{2}} \in Y_h$, $p_h^{n+1} \in M_h$ and $\mathbf{u}_h^{n+1} \in \mathbf{X}_h$ such that $\forall (v_h, \varphi_h, q_h, \mathbf{v}_h) \in Y_h \times Y_h \times Y_h \times \mathbf{X}_h$ there hold

$$\chi\Big(\frac{\phi_h^{n+1}-\phi_h^n}{k}, v_h\Big) - \Big(\widetilde{\phi}_h^{n+\frac{1}{2}}[\beta_1(\widetilde{\phi}_h^{n+\frac{1}{2}})\mathbf{u}_h^n - \beta_2(\widetilde{\phi}_h^{n+\frac{1}{2}})\nabla p_h^n], \nabla v_h\Big) + \Big(\overline{m}(\widetilde{\phi}_h^{n+\frac{1}{2}})\nabla \mu_h^{n+\frac{1}{2}}, \nabla v_h\Big) = 0, \tag{52}$$

$$\frac{1}{2}\Big(\big[(\phi_h^{n+1})^2 + (\phi_h^n)^2\big]\phi_h^{n+\frac{1}{2}}, \varphi_h\Big) - \Big(\widetilde{\phi}_h^{n+\frac{1}{2}} + \mu_h^{n+\frac{1}{2}}, \varphi_h\Big) - \epsilon^2\Big(\nabla\phi_h^{n+\frac{1}{2}}, \nabla\varphi_h\Big) = 0, \tag{53}$$

$$\Big(\frac{1}{2}\nabla(p_h^{n+1}-p_h^n), \nabla q_h\Big) = \frac{ReDa}{\chi k}\Big(\big(\beta_1(\widetilde{\phi}_h^{n+\frac{1}{2}}) - \alpha(\widetilde{\phi}_h^{n+\frac{1}{2}})\beta_2(\widetilde{\phi}_h^{n+\frac{1}{2}})\big)\mathbf{u}_h^n \tag{54}$$
$$- 2\beta_2(\widetilde{\phi}_h^{n+\frac{1}{2}})\big(\nabla p_h^n + \frac{\epsilon^{-1}}{We^*}\widetilde{\phi}_h^{n+\frac{1}{2}}\nabla\mu_h^{n+\frac{1}{2}}\big), \nabla q_h\Big),$$

$$\Big(\frac{ReDa}{\chi k}\mathbf{u}_h^{n+1} + \frac{1}{2}\nabla(p_h^{n+1}-p_h^n), \mathbf{v}_h\Big) = \frac{ReDa}{\chi k}\Big(\big(\beta_1(\widetilde{\phi}_h^{n+\frac{1}{2}}) - \alpha(\widetilde{\phi}_h^{n+\frac{1}{2}})\beta_2(\widetilde{\phi}_h^{n+\frac{1}{2}})\big)\mathbf{u}_h^n \tag{55}$$
$$- 2\beta_2(\widetilde{\phi}_h^{n+\frac{1}{2}})\big(\nabla p_h^n + \frac{\epsilon^{-1}}{We^*}\widetilde{\phi}_h^{n+\frac{1}{2}}\nabla\mu_h^{n+\frac{1}{2}}\big), \mathbf{v}_h\Big).$$

Here one may recall the definitions of β_1, β_2 and $\overline{m}$

$$\begin{aligned}
\beta_1(\widetilde{\phi}_h^{n+\frac{1}{2}}) &= \frac{2ReDa}{2ReDa + \alpha(\widetilde{\phi}_h^{n+\frac{1}{2}})k\chi},\\
\beta_2(\widetilde{\phi}_h^{n+\frac{1}{2}}) &= \frac{k\chi}{2ReDa + \alpha(\widetilde{\phi}_h^{n+\frac{1}{2}})k\chi},\\
\overline{m}(\widetilde{\phi}_h^{n+\frac{1}{2}}) &= \frac{m(\widetilde{\phi}_h^{n+\frac{1}{2}})}{Pe} + \beta_2(\widetilde{\phi}_h^{n+\frac{1}{2}})\frac{\epsilon^{-1}}{We^*}(\widetilde{\phi}_h^{n+\frac{1}{2}})^2.
\end{aligned}$$

Eqs. (54) and (55) amount to solving the Darcy equation (36)-(37) using pressure as the primary variable. This formulation is natural for flow in porous media as boundary conditions are usually only available for pressure (hydraulic head) in these applications. One can certainly solve the Darcy equation in the primitive velocity-pressure formulation. These methods have been studied intensively in the context of the classical pressure-correction algorithm for Navier-Stokes equations, cf. [13] and references therein.

One can establish the following proposition.

Proposition 4.1. *The fully discrete scheme* (52)-(55) *is unconditionally stable and satisfies a modified energy law*

$$\Big\{E_h^{n+1}+\frac{\epsilon^{-1}}{4We^*}||\phi_h^{n+1}-\phi_h^n||_{L^2}^2+\frac{\chi}{ReDa}\frac{k^2}{8}||\nabla p_h^{n+1}||_{L^2}^2\Big\} \tag{56}$$
$$-\Big\{E_h^n+\frac{\epsilon^{-1}}{4We^*}||\phi_h^n-\phi_h^{n-1}||_{L^2}^2+\frac{\chi}{ReDa}\frac{k^2}{8}||\nabla p_h^n||_{L^2}^2\Big\}$$
$$\leq -k\frac{\epsilon^{-1}}{PeWe^*}||\sqrt{m}\nabla\mu_h^{n+\frac{1}{2}}||_{L^2}^2-k||\sqrt{\alpha}\overline{\mathbf{u}}_h^{n+\frac{1}{2}}||_{L^2}^2-\frac{\chi\epsilon^{-1}}{4We^*}||\phi_h^{n+1}-2\phi_h^n+\phi_h^{n-1}||_{L^2}^2,$$

where $\overline{\mathbf{u}}_h^{n+\frac{1}{2}}$ *is an auxiliary* L^2 *function defined as*

$$\overline{\mathbf{u}}_h^{n+\frac{1}{2}}:=\beta_1(\widetilde{\phi}_h^{n+\frac{1}{2}})\mathbf{u}_h^n-\beta_2(\widetilde{\phi}_h^{n+\frac{1}{2}})\nabla p_h^n-\beta_2(\widetilde{\phi}_h^{n+\frac{1}{2}})\frac{\epsilon^{-1}}{We^*}\widetilde{\phi}_h^{n+\frac{1}{2}}\nabla\mu_h^{n+\frac{1}{2}}. \tag{57}$$

Proof. We define another auxiliary L^2 function $\overline{\mathbf{u}}_h^{n+1}$ as

$$\overline{\mathbf{u}}_h^{n+1}:=2\overline{\mathbf{u}}_h^{n+\frac{1}{2}}-\mathbf{u}_h^n.$$

It follows from the definition of β_1,β_2 and $\overline{\mathbf{u}}_h^{n+\frac{1}{2}}$ that

$$\overline{\mathbf{u}}_h^{n+1}=\big(\beta_1(\widetilde{\phi}_h^{n+\frac{1}{2}})-\alpha(\widetilde{\phi}_h^{n+\frac{1}{2}})\beta_2(\widetilde{\phi}_h^{n+\frac{1}{2}})\big)\mathbf{u}_h^n-2\beta_2(\widetilde{\phi}_h^{n+\frac{1}{2}})\big(\nabla p_h^n+\frac{\epsilon^{-1}}{We^*}\widetilde{\phi}_h^{n+\frac{1}{2}}\nabla\mu_h^{n+\frac{1}{2}}\big). \tag{58}$$

Moreover, one has that

$$\frac{ReDa}{\chi}\frac{\overline{\mathbf{u}}^{n+1}-\mathbf{u}_h^n}{k}+\alpha(\widetilde{\phi}_h^{n+\frac{1}{2}})\overline{\mathbf{u}}_h^{n+\frac{1}{2}}+\nabla p_h^n+\frac{\epsilon^{-1}}{We^*}\widetilde{\phi}_h^{n+\frac{1}{2}}\nabla\mu_h^{n+\frac{1}{2}}=0. \tag{59}$$

Now by using the auxiliary functions $\overline{\mathbf{u}}_h^{n+1},\overline{\mathbf{u}}_h^{n+\frac{1}{2}}$, one can equivalently express the Eqs. (52)-(55) as

$$\chi\Big(\frac{\phi_h^{n+1}-\phi_h^n}{k},v_h\Big)-\Big(\widetilde{\phi}_h^{n+\frac{1}{2}}\overline{\mathbf{u}}_h^{n+\frac{1}{2}},\nabla v_h\Big)+\frac{1}{Pe}\Big(m(\widetilde{\phi}_h^{n+\frac{1}{2}})\nabla\mu_h^{n+\frac{1}{2}},\nabla v_h\Big)=0, \tag{60}$$

$$\frac{1}{2}\Big(\big[(\phi_h^{n+1})^2+(\phi_h^n)^2\big]\phi_h^{n+\frac{1}{2}},\varphi_h\Big)-\Big(\widetilde{\phi}_h^{n+\frac{1}{2}}+\mu_h^{n+\frac{1}{2}},\varphi_h\Big)-\epsilon^2\Big(\nabla\phi_h^{n+\frac{1}{2}},\nabla\varphi_h\Big)=0, \tag{61}$$

$$\Big(\frac{1}{2}\nabla(p_h^{n+1}-p_h^n)-\frac{ReDa}{\chi k}\overline{\mathbf{u}}_h^{n+1},\nabla q_h\Big)=0, \tag{62}$$

$$\Big(\frac{ReDa}{\chi}\frac{\mathbf{u}_h^{n+1}-\overline{\mathbf{u}}_h^{n+1}}{k}+\frac{1}{2}\nabla(p_h^{n+1}-p_h^n),\mathbf{v}_h\Big)=0. \tag{63}$$

Now one recognizes that the Eqs. (59)-(60) are the finite element formulation for the semi-discrete scheme (29)-(32). By assumption $\nabla Y_h \subset \mathbf{X}_h$, it follows from Eqs. (62) and (63) that

$$\left(\mathbf{u}_h^{n+1}, \nabla q_h\right) = 0, \quad \forall q_h \in Y_h. \tag{64}$$

In addition, we are allowed to take the test function $\mathbf{v}_h = \frac{k^2}{2}\nabla p_h^n$ in Eq. (63), thanks to the compatibility condition $\nabla Y_h \subset \mathbf{X}_h$. Hence the proof of the modified energy law (56) is exactly the same as the proof of the energy law (42) in Theorem 2.1. □

References

[1] S. Aland, *Time integration for diffuse interface models for two-phase flow*, J. Comput. Phys., 262 (2014), pp. 58–71.

[2] D. M. Anderson, G. B. McFadden, and A. A. Wheeler, *Diffuse-interface methods in fluid mechanics*, in Annual review of fluid mechanics, Vol. 30, vol. 30 of Annu. Rev. Fluid Mech., Annual Reviews, Palo Alto, CA, 1998, pp. 139–165.

[3] A. Baskaran, J. S. Lowengrub, C. Wang, and S. M. Wise, *Convergence analysis of a second order convex splitting scheme for the modified phase field crystal equation*, SIAM J. Numer. Anal., 51 (2013), pp. 2851–2873.

[4] J. Bear, *Dynamics of fluids in porous media*, Courier Dover Publications, Sep 1,1988.

[5] N. Chemetov and W. Neves, *The generalized Buckley-Leverett system: solvability*, Arch. Ration. Mech. Anal., 208 (2013), pp. 1–24.

[6] C. Collins, J. Shen, and S. M. Wise, *An efficient, energy stable scheme for the Cahn-Hilliard-Brinkman system*, Commun. Comput. Phys., 13 (2013), pp. 929–957.

[7] S. Dong and J. Shen, *A time-stepping scheme involving constant coefficient matrices for phase-field simulations of two-phase incompressible flows with large density ratios*, Journal of Computational Physics, 231 (2012), pp. 5788 – 5804.

[8] D. J. Eyre, *Unconditionally gradient stable time marching the Cahn-Hilliard equation*, in Computational and mathematical models of microstructural evolution (San Francisco, CA, 1998), vol. 529 of Mater. Res. Soc. Sympos. Proc., MRS, Warrendale, PA, 1998, pp. 39–46.

[9] X. Feng, *Fully discrete finite element approximations of the Navier-Stokes-Cahn-Hilliard diffuse interface model for two-phase fluid flows*, SIAM J. Numer. Anal., 44 (2006), pp. 1049–1072 (electronic).

[10] X. Feng and S. Wise, *Analysis of a Darcy-Cahn-Hilliard diffuse interface model for the Hele-Shaw flow and its fully discrete finite element approximation*, SIAM J. Numer. Anal., 50 (2012), pp. 1320–1343.

[11] G. Grün, *On convergent schemes for diffuse interface models for two-phase flow of incompressible fluids with general mass densities*, SIAM J. Numer. Anal., 51 (2013), pp. 3036–3061.

[12] J. L. Guermond, P. Minev, and Jie Shen, *An overview of projection methods for incompressible flows*, Comput. Methods Appl. Mech. Engrg., 195 (2006), pp. 6011–6045.

[13] J. L. Guermond and L. Quartapelle, *On the approximation of the unsteady Navier-Stokes equations by finite element projection methods*, Numer. Math., 80 (1998), pp. 207–238.

[14] J. L. Guermond and A. Salgado, *A splitting method for incompressible flows with variable density based on a pressure Poisson equation*, J. Comput. Phys., 228 (2009), pp. 2834–2846.

[15] R. Guo, Y. Xia, and Y. Xu, *An efficient fully-discrete local discontinuous Galerkin method for the Cahn-Hilliard-Hele-Shaw system*, J. Comput. Phys., 264 (2014), pp. 23–40.

[16] Z. Guo, P. Lin, and J. S. Lowengrub, *A numerical method for the quasi-incompressible Cahn-Hilliard-Navier-Stokes equations for variable density flows with a discrete energy law*, J. Comput. Phys., 276 (2014), pp. 486–507.

[17] D. Han, *A decoupled unconditionally stable numerical scheme for the Cahn-Hilliard-Hele-Shaw system*, Journal of Scientific Computing, (2015), pp. 1–20.

[18] D. Han and X. Wang, *Initial-boundary layer associated with the nonlinear Darcy-Brinkman system*, J. Differential Equations, 256 (2014), pp. 609–639.

[19] ——, *A second order in time, uniquely solvable, unconditionally stable numerical scheme for Cahn–Hilliard–Navier–Stokes equation*, J. Comput. Phys., 290 (2015), pp. 139–156.

[20] D. Han, X. Wang, and H. Wu, *Existence and uniqueness of global weak solutions to a Cahn–Hilliard–Stokes–Darcy system for two phase incompressible flows in karstic geometry*, J. Differential Equations, 257 (2014), pp. 3887–3933.

[21] F. Hecht, *New development in freefem++*, J. Numer. Math., 20 (2012), pp. 251–265.

[22] Z. Hu, S. M. Wise, C. Wang, and J. S. Lowengrub, *Stable and efficient finite-difference nonlinear-multigrid schemes for the phase field crystal equation*, J. Comput. Phys., 228 (2009), pp. 5323–5339.

[23] J. Jiang, H. Wu, and S. Zheng, *Well-posedness and long-time behavior of a non-autonomous cahnhilliarddarcy system with mass source modeling tumor growth*, Journal of Differential Equations, (2015), pp. –.

[24] D. Kay, V. Styles, and R. Welford, *Finite element approximation of a Cahn-Hilliard-Navier-Stokes system*, Interfaces Free Bound., 10 (2008), pp. 15–43.

[25] J. Kim, K. Kang, and J. Lowengrub, *Conservative multigrid methods for Cahn-Hilliard fluids*, J. Comput. Phys., 193 (2004), pp. 511–543.

[26] M. Le Bars and M. Grae Worster, *Interfacial conditions between a pure fluid and a porous medium: implications for binary alloy solidification*, J. Fluid Mech., 550 (2006), pp. 149–173.

[27] H.-G. Lee, J. S. Lowengrub, and J. Goodman, *Modeling pinchoff and reconnection in a Hele-Shaw cell. I. The models and their calibration*, Phys. Fluids, 14 (2002), pp. 492–513.

[28] ——, *Modeling pinchoff and reconnection in a Hele-Shaw cell. II. Analysis and simulation in the nonlinear regime*, Phys. Fluids, 14 (2002), pp. 514–545.

[29] J. Lowengrub, E. Titi, and K. Zhao, *Analysis of a mixture model of tumor growth*, European J. Appl. Math., 24 (2013), pp. 691–734.

[30] J. Lowengrub and L. Truskinovsky, *Quasi-incompressible Cahn-Hilliard fluids and topological transitions*, R. Soc. Lond. Proc. Ser. A Math. Phys. Eng. Sci., 454 (1998), pp. 2617–2654.

[31] F. Magaletti, F. Picano, M. Chinappi, L. Marino, and C. M. Casciola, *The sharp-interface limit of the Cahn-Hilliard-Navier-Stokes model for binary fluids*, Journal of Fluid Mechanics, 714 (2013), pp. 95–126.

[32] S. Minjeaud, *An unconditionally stable uncoupled scheme for a triphasic Cahn-Hilliard/Navier-Stokes model*, Numer. Methods Partial Differential Equations, 29 (2013), pp. 584–618.

[33] D. A. Nield and A. Bejan, *Convection in porous media*, Springer-Verlag, New York, second ed., 1999.

[34] J. Shen, *Modeling and numerical approximation of two-phase incompressible flows by a phase-field approach*, in Multiscale modeling and analysis for materials simulation, vol. 22 of Lect. Notes Ser. Inst. Math. Sci. Natl. Univ. Singap., World Sci. Publ., Hackensack, NJ, 2012, pp. 147–195.

[35] J. Shen, C. Wang, X. Wang, and S. M. Wise, *Second-order convex splitting schemes for gradient flows with Ehrlich-Schwoebel type energy: application to thin film epitaxy*, SIAM J. Numer. Anal., 50 (2012), pp. 105–125.

[36] J. Shen and X. Yang, *A phase-field model and its numerical approximation for two-phase incompressible flows with different densities and viscosities*, SIAM J. Sci. Comput., 32 (2010), pp. 1159–1179.

[37] J. Shen and X. Yang, *Decoupled, energy stable schemes for phase-field models of two-phase incompressible flows*, SIAM Journal on Numerical Analysis, 53 (2015), pp. 279–296.

[38] J. Shen, X. Yang, and H. Yu, *Efficient energy stable numerical schemes for a phase field moving contact line model*, Journal of Computational Physics, 284 (2015), pp. 617 – 630.

[39] J. van Kan, *A second-order accurate pressure-correction scheme for viscous incompressible flow*, SIAM J. Sci. Statist. Comput., 7 (1986), pp. 870–891.

[40] X. Wang and H. Wu, *Long-time behavior for the Hele-Shaw-Cahn-Hilliard system*, Asymptot. Anal., 78 (2012), pp. 217–245.

[41] X. Wang and Z. Zhang, *Well-posedness of the Hele-Shaw-Cahn-Hilliard system*, Ann. Inst. H. Poincaré Anal. Non Linéaire, 30 (2013), pp. 367–384.

[42] S. M. Wise, *Unconditionally stable finite difference, nonlinear multigrid simulation of the Cahn-Hilliard-Hele-Shaw system of equations*, J. Sci. Comput., 44 (2010), pp. 38–68.

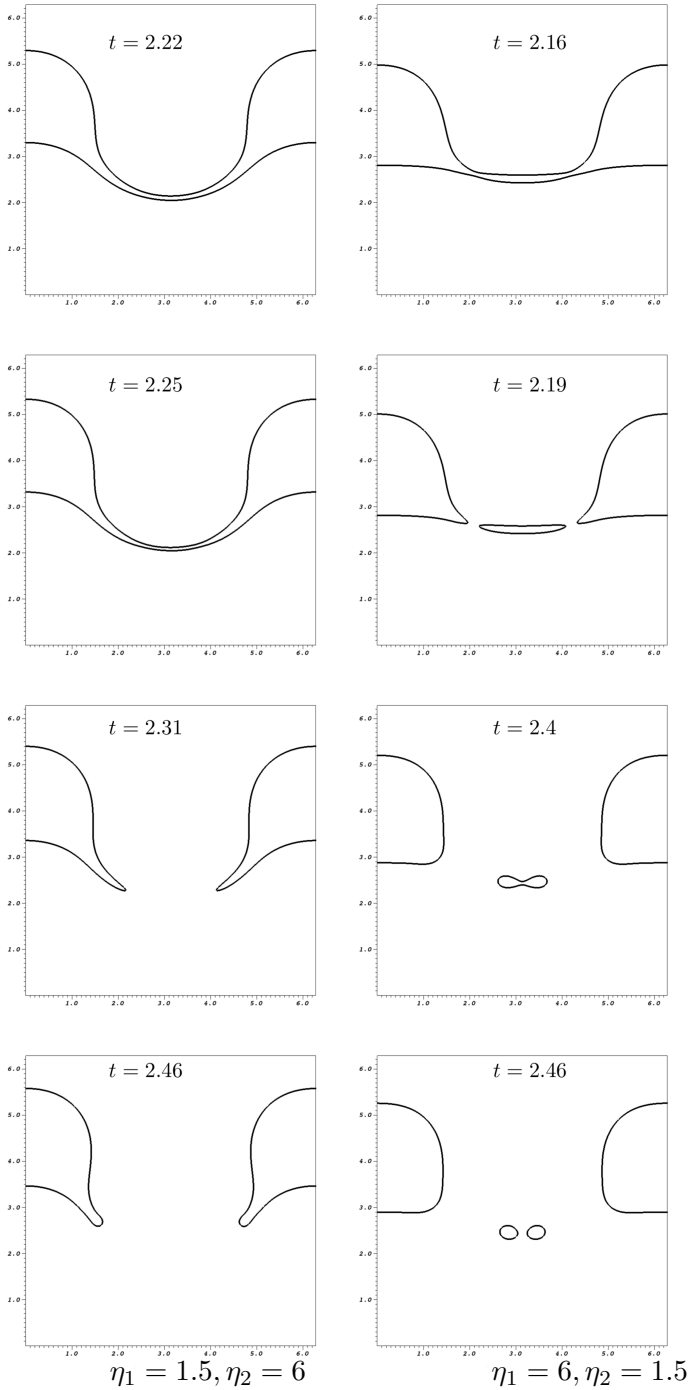

Figure 6: Zero contour plots of the order parameter with mismatched viscosity. The viscosity in the middle layer is η_2, and the viscosity of the rest fluid is η_1. Left column, $\eta_1 = 1.5, \eta_2 = 6$; Right column, $\eta_1 = 6, \eta_2 = 1.5$. The other parameters are the same as before.